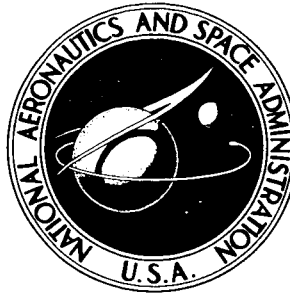


NASA TECHNICAL NOTE



NASA TN D-3183

NASA TN D-3183

N66-14154

FACILITY FORM 602

(ACCESSION NUMBER) <u>21</u>	(THRU) <u>3</u>
(PAGES)	(CODE) <u>33</u>
(NASA CR OR TMX OR AD NUMBER)	(CATEGORY)

GPO PRICE \$ _____

CFSTI PRICE(S) \$ 1.00

Hard copy (HC) _____

Microfiche (MF) .50

ff 653 July 65

EXPERIMENTAL INVESTIGATION OF NOZZLE CRITICAL FLOW CHARACTERISTICS OF SODIUM VAPOR

by Stanley M. Nosek and Louis J. Goldman

Lewis Research Center

Cleveland, Ohio

**EXPERIMENTAL INVESTIGATION OF NOZZLE CRITICAL
FLOW CHARACTERISTICS OF SODIUM VAPOR**

By Stanley M. Nosek and Louis J. Goldman

Lewis Research Center
Cleveland, Ohio

NATIONAL AERONAUTICS AND SPACE ADMINISTRATION

For sale by the Clearinghouse for Federal Scientific and Technical Information
Springfield, Virginia 22151 - Price \$1.00

EXPERIMENTAL INVESTIGATION OF NOZZLE CRITICAL FLOW CHARACTERISTICS
OF SODIUM VAPOR

by Stanley M. Nosek and Louis J. Goldman

Lewis Research Center

SUMMARY

Critical flow rates and pressure ratios of sodium vapor through an axisymmetrical convergent-divergent nozzle were measured to determine the characteristics of the flow process. The vapor flows were measured from condensate flows by a volumetric measurement technique whereby the condensate, at steady-state conditions, was allowed to flow into an auxiliary tank and the rise in level between two electrical resistance-type probes was timed. Pressures at the inlet and the throat of the nozzle were measured with an inert-gas injection technique.

Flows at nozzle inlet pressures from approximately 5 to 13.5 pounds per square inch absolute at saturation temperatures and with up to 100° of superheat were investigated. The receiving (condenser) pressure was maintained low enough to allow complete expansion through the supersonic nozzle.

The measured flows without superheat, expressed per unit of nozzle throat area and corrected for a flow coefficient C_d of 0.97, could be reasonably expressed by $w/A_t C_d = 39.4 p_0$ where w is the weight flow, A_t is the area of the nozzle throat, and p_0 is the nozzle inlet pressure. Comparison of the results with theoretical one-dimensional flow for an isentropic process obeying $p v^n = c$ where p is the absolute pressure, v is the specific volume, n is the process expansion index, and c is a constant indicated that the saturated flows could be represented by an n value of about 1.3. The expansion indexes derived from critical pressure ratios agreed favorably with those derived from flow measurements. Addition of superheat caused a gradual decrease in flow but to the degree applied did not cause a change that might be interpreted as due to the point of condensation shifting from upstream to downstream of the throat.

Comparison of results with theoretical flows for an equilibrium process and a supersaturated-frozen process showed closer agreement with those for an equilibrium process. A calculation for the process wherein the vapor is supersaturated but the molecular species are in equilibrium indicated, however, that a process of this nature may be the best model for representing the flow.

INTRODUCTION

A knowledge of the flow characteristics of alkali metal vapors under rapidly expanding conditions is of practical interest in the design of turbines for space power Rankine systems. In particular, it is necessary to have an accurate knowledge of the expansion process to properly size the flow passages. Without this knowledge, two choices for the process have been usually considered, which most probably provide the boundaries of flow predictable by existing thermodynamic data. One is the equilibrium expansion process, in which the expansion is assumed to occur with equilibrium both between physical phases of vapor and liquid and among chemical reaction species of monatomic and polyatomic molecules. The second choice is a supersaturated-frozen expansion in which it is assumed that condensation is delayed so that the fluid remains vaporous throughout the expansion. It is further assumed that the expansion proceeds too rapidly to allow any change in the chemical composition from the initial state point (the composition remains frozen) so that the molecular weight remains constant. The vapor is presumed to behave as an ideal gas. The theoretically calculated flow between the two processes, as shown in reference 1, is significantly different; consequently, a more accurate identification of the expansion process is required.

In references 2 and 3, from flows through nozzles as measured with electromagnetic flowmeters, it was indicated that the supersaturated process was more plausible for approximating the critical flow of sodium vapor. Both investigations, however, left a more accurate identification of the process still to be desired. In reference 4, on the basis of accurate pressure measurements along a convergent-divergent nozzle and the assumptions that the flow was isentropic and obeyed the equation $pv^n = c$, it was found that an expansion index n of 1.3 best represented the experimental data. Comparison with equilibrium and supersaturated processes on the same assumptions would indicate that the actual process was between the two.

To provide further evidence toward identification of the process, the facility in references 3 and 4 was modified and operated to obtain more accurate nozzle flow measurements. The results are the subject of this report. A volumetric flow measuring technique was incorporated whereby the condensate was allowed to flow into a tank and the rise between level probes was timed. Flows were measured over a range of nozzle inlet pressures from approximately 5 to 13.5 pounds per square inch absolute at saturation temperatures and with up to 100° of indicated superheat. The condenser pressure was maintained from 1 to 3.5 pounds per square inch absolute to provide supersonic flow through the nozzle.

In addition to the flows, the pressures at the inlet and throat of the nozzle were measured with the injection technique described in reference 4. The measured flows at saturated conditions are compared with theoretical curves of flow calculated on the same assumptions as in reference 4, that is, that the vapor flows isentropically and obeys $pv^n = c$. Theoretical curves for equilibrium and supersaturated processes were also calculated for comparison. Expansion indexes were derived from the measured nozzle throat to inlet pressure ratios and are compared with those determined on the basis of flow. The effect of superheat on flow characteristics is also noted.

SYMBOLS

A	area, sq in.
C_d	nozzle flow coefficient
c	constant
g	gravitational constant, 32.17 ft/sec ²
n	process expansion index
p	absolute pressure, psia
T	temperature, °F or °R
v	specific volume, lb/cu ft
w	weight flow, lb/hr
γ	ratio of specific heat at constant pressure to specific heat at constant volume

Subscripts:

o	nozzle inlet
t	throat of nozzle

APPARATUS AND INSTRUMENTATION

The investigation covered by this report was conducted in the sodium flash-vaporization facility and research nozzle assembly described in references 3 and 4. To carry out the research reported herein, the facility was modified by adding a condensate flow measuring tank, herein identified as a volumeter. In addition, a larger demister was incorporated into the separator, and a swirler was inserted into the superheater section between the separator and the nozzle.

Vapor Generation System

The vapor generation system is shown schematically in figure 1, where the major components and peak design parameters are indicated. The vapor and equivalent condensate flow peak value were corrected to show 200 pounds per hour rather than 300 pounds per hour as indicated in figure 1 of reference 4 to be more consistent with the actual peak value attained. The system design and components are described in detail in reference 3.

The larger demister was deemed to be necessary as a result of the previous investigation (ref. 4) in which the dryness of the vapors leaving the separator

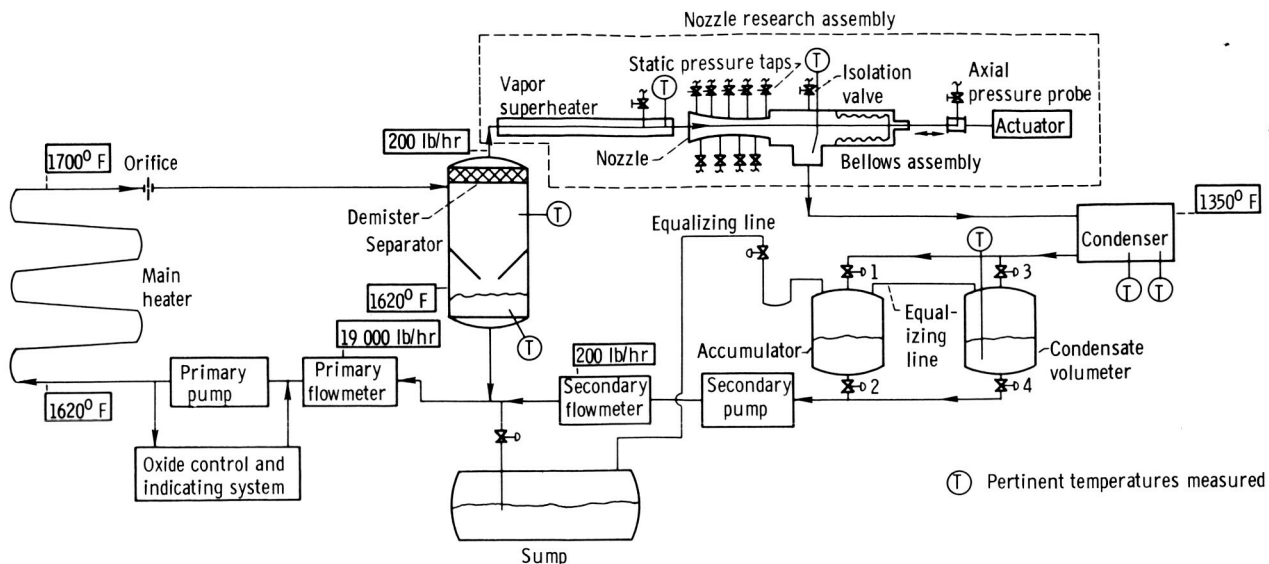


Figure 1. - Schematic of sodium flash-vaporization facility.

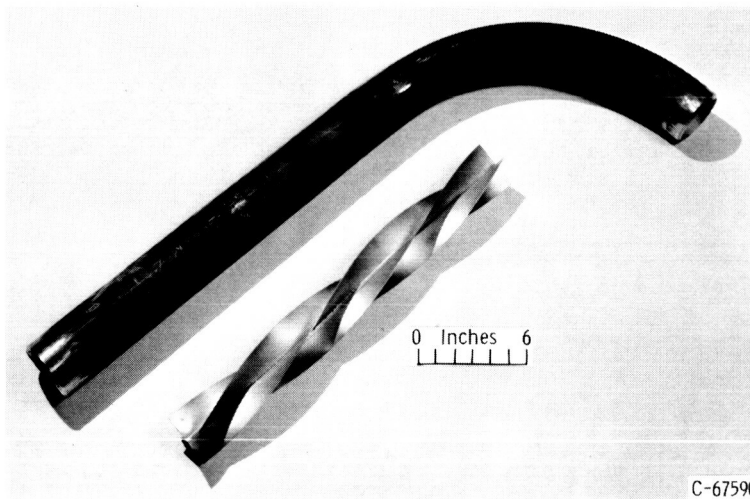


Figure 2. - Swirler and superheater inlet section.

appeared doubtful. The original demister was a section of 4-inch pipe filled with stainless-steel wire mesh to a depth of approximately 4 inches extending into the end cap of the 14-inch-diameter tank. The end cap was cut off and a section of 14-inch pipe, approximately 10 inches in length and completely filled with mesh, was added. A new end cap, with the mouth of the 3-inch discharge pipe welded flush with the inside surface, was welded on the demister section.

The swirler was added to augment the demisting and superheat capabilities. It was fabricated from 20-gage stainless-steel sheet to form four perpendicular vanes and then twisted to provide approximately 270° of swirl. The swirler was approximately 2 feet long and fit snugly into the 3-inch discharge pipe from the separator. A photograph of the swirler and pipe is shown in figure 2.

Research Nozzle

The nozzle research assembly is included schematically in figure 1. Complete details of the assembly and pressure measuring technique are presented in reference 4. The axial pressure probe was in place, as indicated, but was not utilized in this investigation. The nozzle is axisymmetrical and convergent-divergent. The convergent section is elliptical in contour and fairs at about 1/4 inch downstream of the throat into a conical divergent section. At the throat, the contour is flat for 0.030 inch. The inlet diameter is 3.06 inches, the throat diameter is 0.677, and the outlet diameter is 0.845. The length from inlet to outlet is 3.75 inches with the throat $2\frac{1}{2}$ inches from the inlet. The area of the throat minus the area of the 1/8-inch-diameter probe over the range of nozzle inlet temperatures investigated was calculated to be 0.3573 ± 0.0006 square inch.

Condensate Volumeter

The condensate volumeter for measuring the vapor flow through the research nozzle consisted of a tank nominally 8 inches in diameter and 25 inches long installed in parallel with the accumulator as shown in figure 1. Remotely operated valves were included, as shown, to manually direct the flow as required. A schematic drawing of the volumeter with pertinent dimensions is shown in figure 3. Installed in the volumeter were a low-level and a high-level electrical resistance-type probe between which the rise in level was timed. The volume between the probes as calculated from the dimensions, corrected for thermal growth at selected condensate temperatures, is listed in figure 3. The top of the tank was flat to facilitate the installation and accurate positioning of the probes. The probes were designed on principles set forth in reference 5. The electrical resistance type was used in preference to the spark plug type in order to circumvent the problem of shorting out due to condensation on the probe.

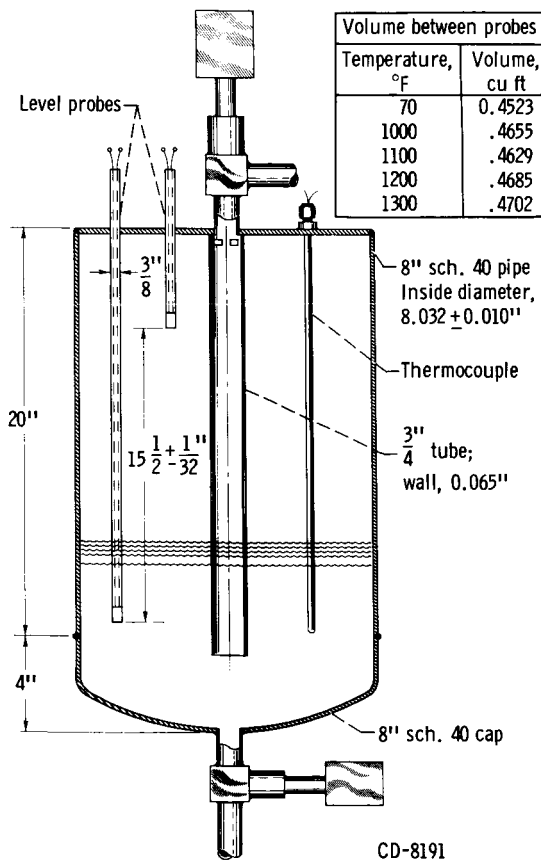


Figure 3. - Schematic drawing of condensate volumeter.

Instrumentation

Only instrumentation - temperature, pressure, and flow - pertinent to this investigation will be presented here. Those necessary for operation and control of the facility are presented in reference 3.

Temperature measurement. - Temperatures were measured with Chromel-Alumel thermocouples at locations indicated in figure 1. Two immersed in-well thermocouples were used in the separator, one in the liquid at the bottom, the other in the vapor near the top. Both agreed to within 1° or 2° during the course of a run.

The nozzle inlet temperature was measured by a single immersed, sheathed thermocouple located approximately 6 inches upstream of the nozzle inlet. The absolute value from this thermocouple was found to be in error, and therefore it was used only for determining the amount of superheat from changes in its readings. The separator temperature was used as the nozzle inlet temperature at saturated conditions.

The nozzle discharge temperature was measured in the discharge tee with a single immersed, sheathed thermocouple. This temperature was measured for comparison with the condenser temperature to note the degree of superheat attained by the sudden dissipation of the discharge velocity. In the absence of a quality meter, the attainment of superheat at this location would provide some assurance that the quality of the vapors entering the nozzle was high.

The condenser temperature was measured with two immersed, in-well thermocouples located at the bottom header. The back pressure on the nozzle was controlled by this temperature, which was always held low enough to assure critical flow through the nozzle. The temperature in the volumeter was measured with a single, sheathed thermocouple immersed to the depth beyond that of the low-level probe as indicated in figure 3. All temperatures were manually recorded as readout on a selfbalancing potentiometer indicator calibrated in degrees.

Pressure measurement. - Static pressures in the nozzle were measured with wall taps and the inert-gas injection technique described in reference 4. Nine wall taps with 0.020-inch sensing holes were spaced along the nozzle profile. In addition, an inlet pressure tap with a 0.060-inch sensing hole was located about 6 inches upstream of the nozzle and a discharge pressure tap was located in the downstream tee. The throat tap was located at the middle of the 0.030 flat portion of the profile. Only the inlet pressure and the throat pressure were utilized in this investigation. In a few cases, the inlet pressure tap became plugged so in these cases the pressures between the inlet and the throat were used for graphically extrapolating the inlet pressure. The throat tap was always clear.

The pressures were read on a U-tube mercury manometer. The barometric pressure was read on-site by evacuating the manometer. The temperature of the manometer was also read.

Vapor flow measurement technique. - The vapor flow through the nozzle was measured from its equivalent condensate flow, at steady-state conditions, into the volumeter. The value of density that is necessary to convert volumetric rate to weight flow rate was calculated from an equation available in reference 6 or 7. The average temperature of readings taken before, midway, and after a run was used. The time for the level to rise between the level probes was measured with an electric timer and read to 0.001 of a minute. Starting and stop-

ping of the timer was controlled automatically through suitable relays as the liquid made contact with the probes. Indicating lights were also automatically energized as the liquid reached each level.

If the accuracies of the volume between the probes, the density, and the time measured to fill the volume are considered, the flow rate was believed to have been measured to an accuracy well within 1 percent.

RESULTS OF INVESTIGATION

The results of the investigation are presented by a compilation of the experimental data and a graphical analysis of the results in comparison with theoretical models to determine the characteristics of the flow process through the nozzle. With the use of a vapor pressure-temperature relation based on measurements, the flows at saturated conditions are first correlated against nozzle inlet pressure. Comparison of the flow is then made with curves of theoretical flow based on assumed processes of equilibrium, supersaturated-frozen, and $pv^n = c$. A calculation for a supersaturated-equilibrium process is also included. Expansion indexes n derived for the experimental flows are then compared with those derived for the experimental critical pressure ratios. The expansion indexes from the critical pressure ratios for the equilibrium, supersaturated-frozen, and the supersaturated-equilibrium processes are included for comparison. Finally, all of the experimental flows are plotted against nozzle inlet temperature to note the effect of superheat. The theoretical trend for the bounding equilibrium and supersaturated-frozen processes at a representative inlet pressure is used for comparison.

Experimental Data Obtained

The experimental data obtained in this investigation are tabulated in tables I to III. Table I presents the results of all 102 flow runs, and table II presents the averages of the data at each set nozzle inlet condition. Table III presents the results of the pressure measurements. The pertinent temperatures are included in all tables. The flow rates in tables I and II are expressed per unit of throat area and are assumed to be equivalent to vapors entering the nozzle at 100 percent quality. The fact that superheat was attained by the vapors at discharge from the nozzle, which may be noted by comparison of the nozzle discharge and condenser temperatures, indicated that this assumption is reasonable.

In table III the nozzle inlet pressure, which was measured in inches of mercury and corrected for thermal effects, is presented in pounds per square inch absolute. The throat pressure is listed indirectly as a ratio to the inlet pressure since the primary interest was in arriving at the expansion index, which was calculated from

$$\frac{p_t}{p_o} = \left(\frac{2}{n+1} \right)^{n/(n-1)} \quad (1)$$

TABLE I. - NOZZLE VAPOR FLOW RATE DATA

Run	Sepa- rator	Super- heat	Nozzle dis- charge	Condenser outlet	Volu- meter	Vapor flow rate, w/A _t , lb/(hr)(sq in.)	Run	Sepa- rator	Super- heat	Nozzle dis- charge	Condenser outlet	Volu- meter	Vapor flow rate, w/A _t , lb/(hr)(sq in.)
1	1433	0	1214	1200	993	211.2	51	1481	35	1248	1207	1135	271.9
2	1435	0	1210	1195	1050	210.6	52	1481	38	1250	1205	1122	271.4
3	1434	0	1210	1195	1067	209.0	53	1520	0	1268	1254	1190	347.8
4	1433	0	1207	1195	1035	209.6	54	1520	0	1270	1255	1173	349.1
5	1434	0	1210	1197	1022	211.1	55	1564	0	----	----	1230	----
6	1435	0	1210	1197	1067	209.2	56	1564	0	----	----	1193	----
7	1434	0	1210	1194	1017	216.6	57	1565	0	1270	1252	1237	431.2
8	1435	0	1200	1185	1085	209.9	58	1565	0	1275	1260	1250	424.9
9	1520	0	1235	1210	1161	339.7	59	1565	0	1274	1257	1245	428.7
10	1520	0	1235	1210	1153	340.5	60	1598	0	1282	1252	1245	508.0
11	1520	0	1235	1211	1161	339.5	61	1599	0	1281	1252	1237	508.9
12	1520	0	1235	1210	1120	341.0	62	1456	0	1268	1259	1240	229.0
13	1520	0	1235	1210	1120	340.7	63	1456	0	1265	1259	1235	232.0
14	1521	42	1225	1204	1063	334.1	64	1456	0	1265	1255	1235	232.4
15	1521	42	1230	1205	1085	339.7	65	1461	0	1266	1255	1237	238.7
16	1521	40	1315	1302	1153	334.7	66	1461	0	1263	1253	1238	239.7
17	1521	40	1315	1300	1227	310.8	67	1505	0	1268	1255	1255	310.7
18	1521	40	1315	1301	1213	309.1	68	1505	0	1266	1254	1243	309.8
19	1521	40	1315	1301	1227	305.6	69	1505	0	1267	1254	1243	307.6
20	1520	0	1311	1300	1225	319.3	70	1507	77	1332	1273	1258	296.2
21	1519	0	1311	1302	1220	317.8	71	1506	93	1333	1267	1253	296.5
22	1519	0	1312	1302	1145	332.5	72	1506	97	1333	1265	1250	295.8
23	1518	0	1312	1300	1145	320.0	73	1506	24	1288	1265	1248	301.4
24	1516	0	1315	1304	1145	322.4	74	1506	24	1283	1265	1250	301.4
25	1552	0	1317	1305	1227	400.3	75	1506	55	1306	1264	1250	298.2
26	1552	0	1317	1306	1287	399.3	76	1506	57	1306	1264	1245	297.6
27	1551	0	1317	1305	1290	402.0	77	1551	55	1326	1269	1258	380.3
28	1553	0	1316	1304	1287	398.5	78	1551	53	1326	1269	1258	379.9
29	1552	42	1349	1302	1278	384.1	79	1550	18	1299	1270	1262	383.5
30	1552	42	1349	1305	1277	385.6	80	1550	17	1298	1269	1253	382.0
31	1551	41	1349	1305	1288	381.1	81	1550	17	1297	1269	1258	381.4
32	1550	22	1333	1303	1297	379.8	82	1550	0	1284	1269	1260	391.1
33	1550	23	1335	1305	1277	382.2	83	1549	0	1284	1269	1258	384.7
34	1577	0	1320	1305	1293	455.3	84	1549	0	1284	1269	1253	385.9
35	1577	0	1320	1302	1290	455.2	85	1583	0	1280	1263	1250	469.6
36	1580	22	1337	1305	1245	453.9	86	1583	0	1284	1267	1252	469.8
37	1580	22	1335	1303	1240	454.6	87	1461	0	1260	1251	1240	238.0
38	1578	0	1319	1305	1245	464.0	88	1460	0	1260	1251	1240	238.7
39	1578	0	1319	1304	1245	462.4	89	1460	0	1261	1251	1238	236.6
40	1600	0	1325	1308	1245	515.4	90	1459	23	1263	1252	1240	229.3
41	1600	0	1321	1305	1245	518.6	91	1459	23	1260	1251	1238	227.9
42	1600	0	1320	1305	1245	515.1	92	1460	23	1261	1251	1240	227.5
43	1565	0	1320	1305	1300	424.8	93	1461	60	1286	1252	1238	227.3
44	1565	0	1320	1305	1280	424.3	94	1460	61	1287	1251	1238	226.3
45	1565	21	1330	1306	1257	431.0	95	1460	61	1287	1251	1233	220.7
46	1566	20	1334	1305	1230	436.3	96	1460	61	1285	1250	1233	222.3
47	1566	23	1336	1305	1265	432.1	97	1461	100	1300	1252	1240	224.3
48	1566	21	1336	1306	1275	430.8	98	1461	103	1301	1252	1240	223.3
49	1480	0	1223	1206	1142	281.5	99	1599	53	1352	1286	1268	488.7
50	1480	0	1225	1207	1142	281.8	100	1599	53	1349	1282	1263	488.4
							101	1597	0	1296	1281	1257	496.6
							102	1598	0	1297	1282	1260	494.7

TABLE II. - AVERAGE NOZZLE VAPOR FLOW RATE DATA

Run	Sepa- rator	Super- heat	Condenser outlet	Measured, lb/(hr)(sq in.)	Variation of maximum and minimum from average, percent
1 to 8	1434	0	1195	210.9	2.7
9 to 13	1520	0	1210	340.3	-1.0
14 to 15	1521	42	1205	336.9	-.2
16	1521	40	1302	334.7	±.8
17 to 19	1521	40	1301	308.5	0
					.7
					-.9
20 to 21	1520	0	1301	318.6	.2
					-.3
22	1519	0	1302	332.5	0
23 to 24	1517	0	1302	321.2	±.4
25 to 28	1552	0	1305	400.0	.5
					-.4
29 to 31	1552	42	1304	383.6	.5
					-.7
32 to 33	1550	23	1304	381.0	±.3
34 to 35	1577	0	1304	455.3	0
36 to 37	1580	22	1304	454.3	±.1
38 to 39	1578	0	1305	463.2	±.2
40 to 42	1600	0	1306	516.4	.4
					-.3
43 to 44	1565	0	1305	424.6	±.1
45 to 48	1566	21	1306	432.6	.8
					-.4
49 to 50	1480	0	1207	281.7	±.1
51 to 52	1481	37	1206	271.7	±.1
53 to 54	1520	0	1255	348.5	±.2
57 to 59	1565	0	1256	428.3	.7
					-.8
60 to 61	1599	0	1252	508.5	±.1
62 to 64	1456	0	1258	231.1	.6
					-.9
65 to 66	1461	0	1254	239.2	±.2
67 to 69	1505	0	1254	309.4	.4
					-.6
70	1507	77	1273	296.2	0
71 to 72	1506	95	1266	296.2	±.1
73 to 74	1506	24	1265	301.4	0
75 to 76	1506	56	1264	297.9	±.1
77 to 81	1551	54	1269	380.1	±.1
79 to 81	1550	17	1269	382.3	.3
					-.2
82 to 84	1549	0	1269	387.2	1.0
					-.6
85 to 86	1583	0	1265	469.7	0
87 to 89	1460	0	1251	237.8	.4
					-.5
90 to 92	1459	23	1251	228.2	.5
					-.3
93 to 96	1460	61	1251	224.2	1.4
					-1.6
97 to 98	1461	102	1252	223.8	±.2
99 to 100	1599	53	1284	488.6	±.1
101 to 102	1598	0	1282	495.7	±.2

TABLE III. - NOZZLE PRESSURE DATA

Run	Sepa- rator	Super- heat	Nozzle dis- charge	Condenser outlet	Nozzle inlet pressure, p_o , psia	Nozzle throat to inlet pressure ratio, p_t/p_o	Process expansion index, n_t
50A	1480	0	1225	1206	7.06	0.537	1.35
50B	1480	0	1225	1205	7.02	.539	1.34
51	1482	40	1250	1206	^a 7.01	.539	1.34
52	1519	0	1268	1253	^a 8.82	.546	1.30
53A	1521	0	1267	1251	8.83	.548	1.29
53B	1520	0	1267	1252	8.82	.546	1.30
59A	1565	0	1270	1250	11.18	.540	1.33
59B	1566	0	1270	1247	11.12	.546	1.30
59C	1566	0	1270	1249	11.08	.547	1.29
61	1598	0	1279	1244	^a 13.40	.533	1.38
66A	1461	0	1262	1246	^a 6.26	.557	1.24
66B	1462	0	1262	1247	^a 6.26	.559	1.23
69	1505	0	1266	1248	^a 8.07	.549	1.28
72	1506	97	1333	1255	^a 8.12	.542	1.32
74	1506	22	1279	1255	^a 8.02	.551	1.27
76	1507	56	1308	1255	8.06	.543	1.31
78A	1550	56	1325	1265	10.31	.541	1.33
78B	1550	57	1325	1263	10.30	.541	1.33
81	1551	18	1296	1262	10.41	.533	1.37
86A	1584	0	1284	1262	12.45	.536	1.36
86B	1585	0	1284	1263	12.38	.539	1.34
89A	1460	0	1260	1244	6.27	.551	1.27
89B	1460	0	1260	1243	6.29	.543	1.32
92	1460	21	1261	1246	6.30	.542	1.32
96A	1461	64	1287	1243	6.31	.537	1.35
96B	1461	64	1287	1243	6.17	.546	1.30
98A	1461	96	1300	1244	6.20	.540	1.33
98B	1461	98	1300	1243	6.20	.533	1.37
100A	1600	54	1350	1274	13.47	.526	1.41
100B	1600	53	1348	1273	13.53	.529	1.40

^aExtrapolated.

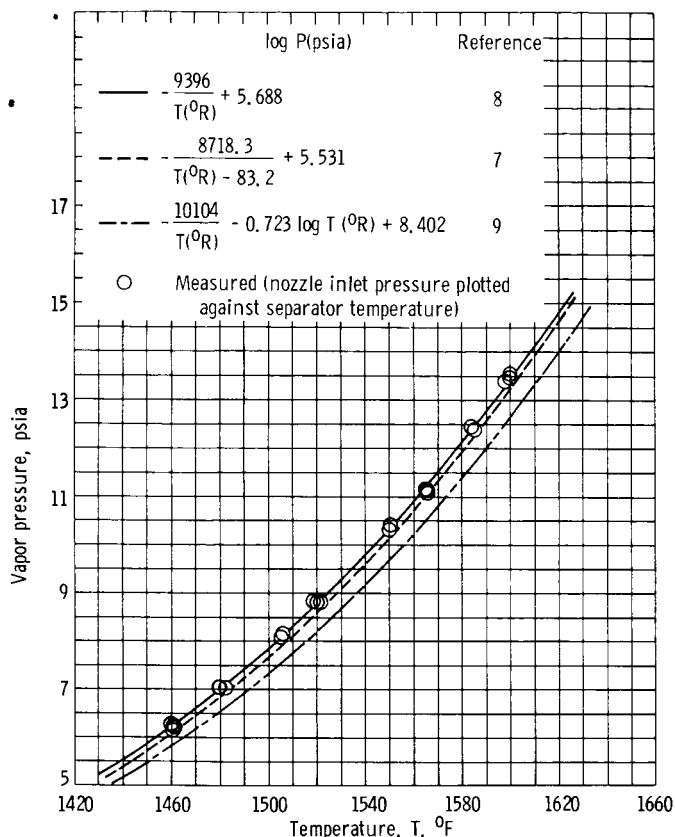


Figure 4. - Saturated vapor pressure - temperature relations.

both flows and pressures were not measured at all inlet conditions. The results also provide a check against vapor pressure curves recommended in references. Excellent agreement was found with the equation from reference 8 so that it could serve as the calibration curve. In comparison with the curve from reference 7, the points fall within 5° , which is within the accuracy, approximately $1/2$ percent, of the temperature measurements. In the previous investigation (ref. 4), where the nozzle inlet temperature was used, close agreement was found with this curve. This provides substantiating evidence that the added demister and swirler did not add significant pressure drop to the vapor flow to the nozzle and that the separator temperature, therefore, may be used as the saturation temperature into the nozzle inlet.

Weight Flow Correlation

The average critical flow rates from table II measured at saturated nozzle inlet conditions are plotted in figure 5 for correlation against nozzle inlet pressure. The pressures were taken from the calibration curve in figure 4. The flows are corrected by a flow coefficient C_d to express the results on a theoretical flow basis for subsequent comparisons. The value of C_d was arrived at from pretest of the nozzle with air at ambient temperature prior to installation in the facility. Over a range of Reynold's numbers at the throat from 7×10^4 to

It is assumed that the critical pressure of the stream at the wall is at the location of the throat pressure tap. The critical pressure ratios are estimated to be $1/2$ to 1 percent accurate, the percent being better at the higher pressures. The expansion index is very sensitive to the pressure ratio, approximately by a factor of three, so the accuracy of the expansion index is from $1\frac{1}{2}$ to 3 percent.

Saturated Vapor Pressure - Temperature Relation

The nozzle inlet pressures and separator temperatures from table III are plotted in figure 4 to arrive at a calibration curve for use in plotting the flow data against pressure. This approach was necessary since the flow and pressure could not be measured simultaneously and also for the reason that

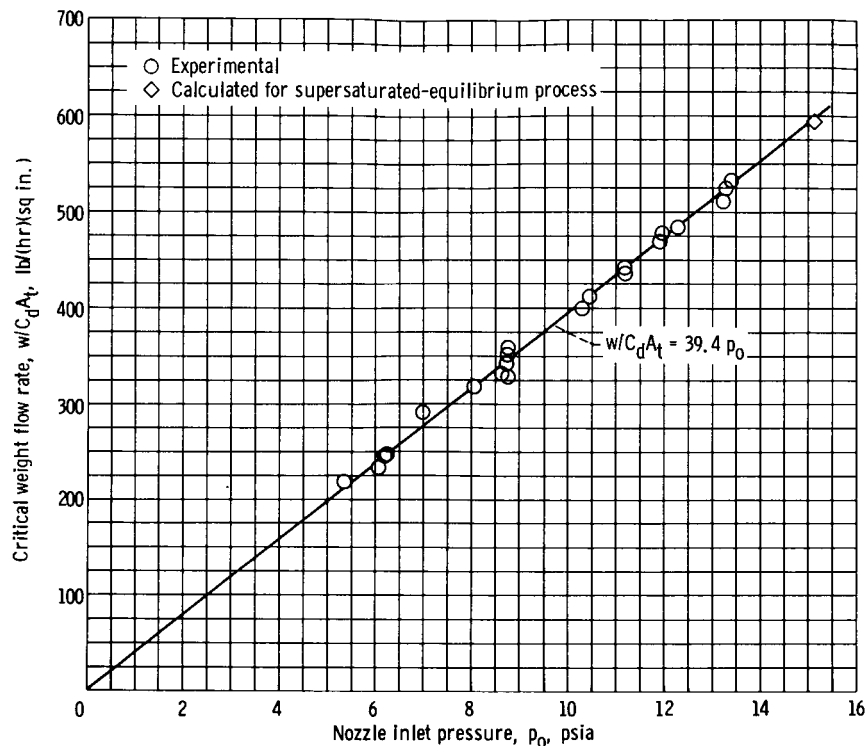


Figure 5. - Variation of experimental critical vapor flow rates with nozzle inlet pressure.

22×10^4 , the flow coefficient ranged from 0.971 to 0.977. It was estimated, using viscosity data from reference 6 for saturated vapor, that the Reynold's number would range from 3×10^4 to 8×10^4 for the conditions investigated herein. A constant flow coefficient of 0.97 was therefore considered reasonable to assume.

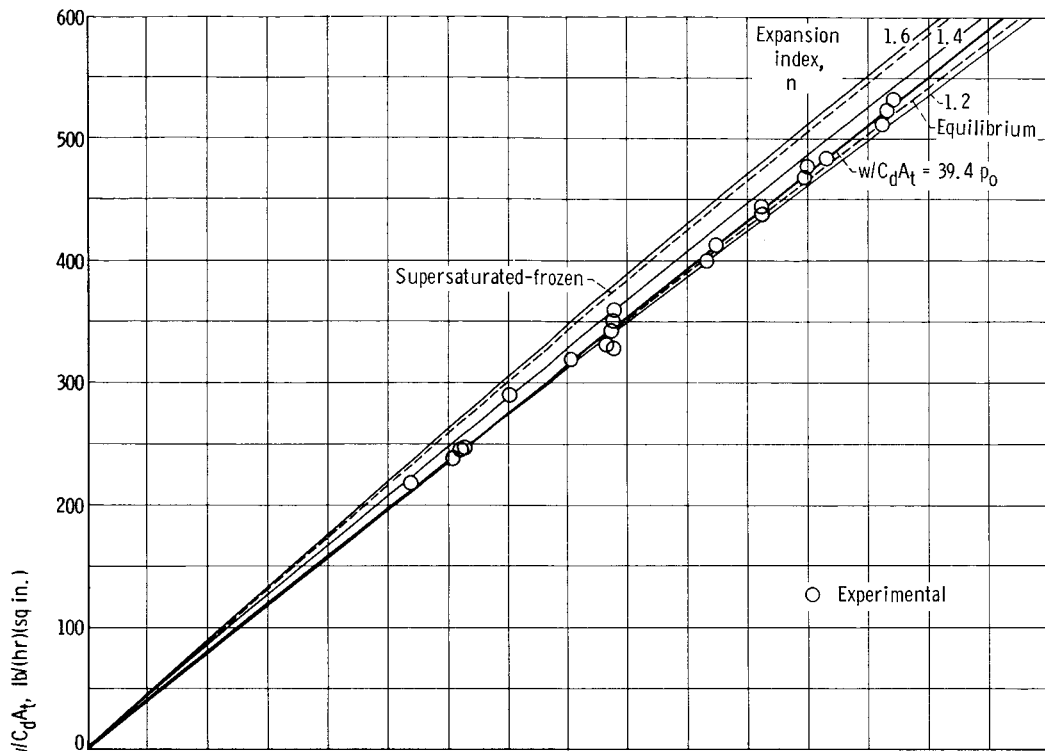
It is seen in figure 5 that the least-squares line

$$\frac{w}{C_d A_t} = 39.4 p_0$$

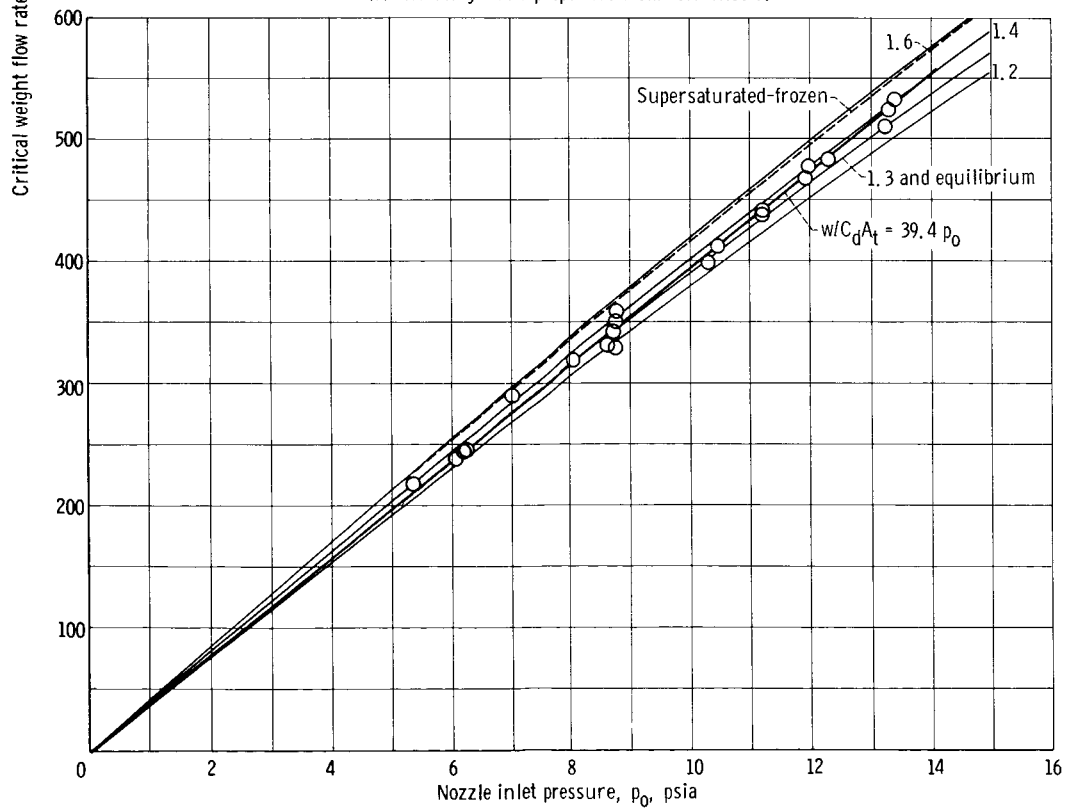
through the points provides a reasonable representation of the flow. Deviations from the line are within ± 2 percent at pressures above 9 pounds per square inch and up to ± 5 percent at pressures below 9 pounds per square inch. The deviations would have been less, perhaps, had it been possible to factor in the actual quality of the vapor.

Comparison of Experimental Flow with Theoretical Flow

In figure 6, the flows are compared with theoretically calculated flows. Since, at present, there is not a definitive set of thermodynamic data for the range of conditions investigated herein, three sources were considered (refs. 7 to 9) for the theoretical calculations. In figure 6(a), properties from reference 7 were used. In figure 6(b), properties from reference 8 were used; and in figure 6(c), properties from reference 9 were used. Differences in the sets

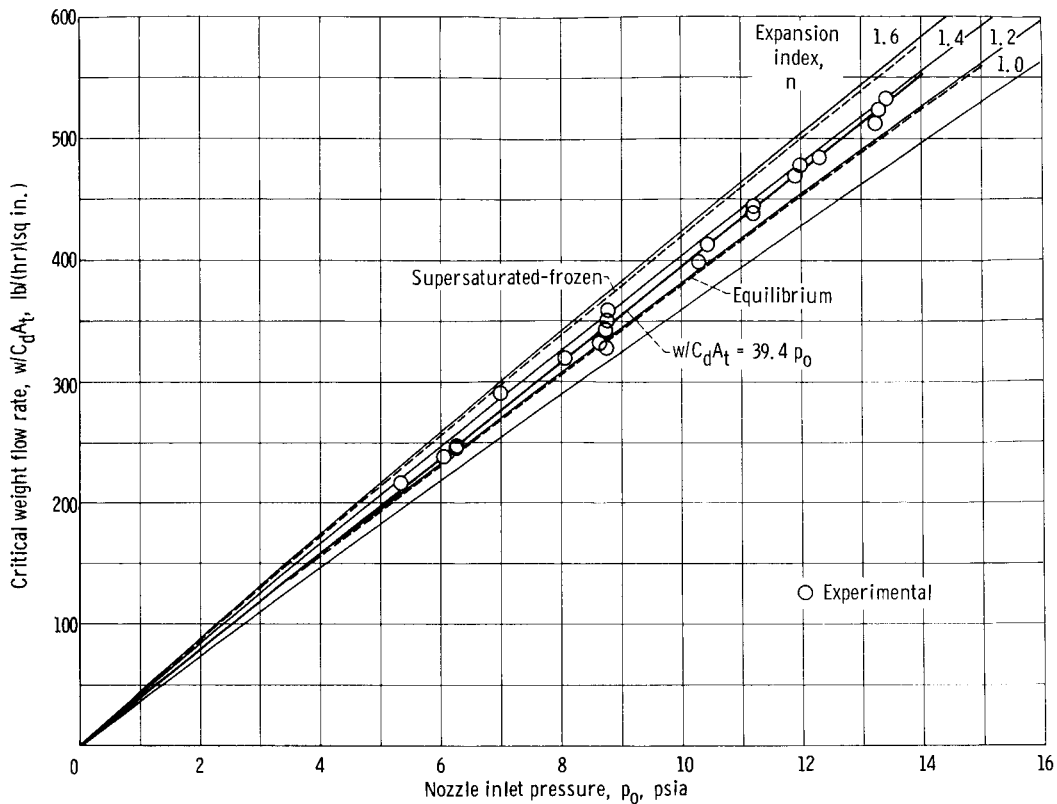


(a) Thermodynamic properties from reference 7.



(b) Thermodynamic properties from reference 8.

Figure 6. - Variation of critical vapor flow with nozzle inlet pressure.



(c) Thermodynamic properties from reference 9.

Figure 6. - Concluded.

of properties arise from the heat of dimerization value and the vapor pressure curve assumed. The heat of dimerization values are -18 200 calories per gram mole Na_2 in reference 7, -16 840 in reference 8, and -17 500 in reference 9. The differences in vapor pressure curves are shown in figure 4, where it may be noted that the pressures from references 7 and 8 are reasonably close to each other and to the pressures measured in this investigation, whereas the pressures from reference 9 are substantially lower.

The theoretical flows shown by the solid lines in figure 6 were calculated on the same basis as in reference 4; that is, the flow is assumed to be one-dimensional and isentropic and obeys the equation $p v^n = c$. Based on these assumptions, the following equation for critical flow may be derived:

$$\frac{w}{C_d A_t} = 300 \left[g n \left(\frac{2}{n+1} \right)^{(n+1)/(n-1)} \frac{p_0}{v_0} \right]^{1/2} \quad (2)$$

from which a family of curves with selected values of n was calculated and plotted as shown.

Compared with these curves, it is seen in figure 6 that the experimental results can be reasonably represented by equation (2) with a constant value of n over the pressure range, the value being dependent on the source of proper-

ties used. In figure 6(a), with properties from reference 7, the n value, by inspection, is about 1.25; in figure 6(b) with properties from reference 8, it is about 1.35; in figure 6(c), with properties from reference 9, it is about 1.33, or nominally 1.3 in all cases.

Theoretical flows were calculated also for the two processes, described in the INTRODUCTION, with are usually considered for turbine design: (1) the equilibrium process, and (2) the supersaturated-frozen process. The procedure for calculating equilibrium flow rates was the same as that outlined in reference 3, that is, finding the maximum ratio of velocity to specific volume along an isentropic process using tabulated equilibrium thermodynamic properties. The critical flow rates for the supersaturated-frozen case were calculated directly from equation (2) with the ratio of specific heat at constant pressure to the specific heat at constant volume γ at the inlet condition used for the expansion index n . References 7 and 8 do not provide values of γ ; therefore, the specific heat values in reference 10 for monomer and dimer species were used in conjunction with molecular compositions from references 7 and 8 to calculate the values. The resulting flows for these two processes are shown in figure 6 by the dashed lines. In figures 6(a) and (b), the equilibrium process is a much closer approximation of the flow; while in figure 6(c), neither one is reasonably close.

Another model that may be considered for comparison is one based on a supersaturated-equilibrium process. In this process the vapor expands supersaturated with the molecular species in equilibrium so that the molecular weight changes during the expansion. A calculation was made in this case with data from reference 11 at an inlet temperature of 1625° F (15.18 psia), which is the lowest temperature at which properties in this reference are available. An n value was derived for this process and the flow was determined from equation (2). The result of the calculation is shown in figure 5 (p. 12) where it falls practically on the least-squares line.

Comparison of Expansion Indexes from Flow and Critical Pressure Ratios

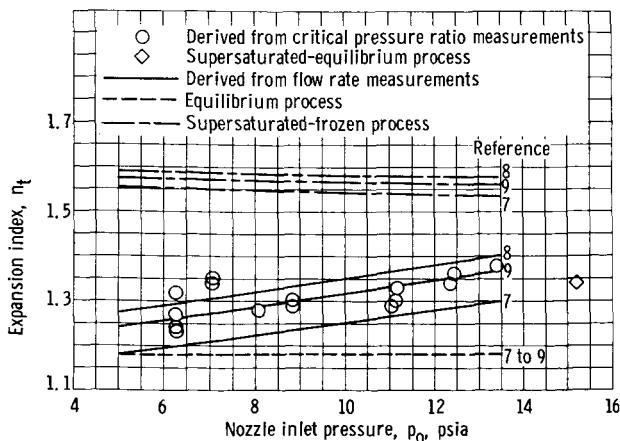


Figure 7. - Variation of expansion index with nozzle inlet pressure.

If it is assumed that the least-squares line is a better representation of the flow than equation (1) with a constant value of n and the least-squares line is equated to equation (2), values of n as a function of inlet pressure may be derived. The resulting n values were essentially linear with inlet pressure and are shown by the solid lines in figure 7, where the range of values (1.18 to 1.28 at 5 psia and 1.3 to 1.4 at 13.5 psia), again, depends on the properties

used. The n values calculated from the critical pressure ratio measurements are also plotted and substantiate the increasing trend with inlet pressure. Agreement is closest with the use of properties from reference 9, although considering the accuracy of the data, the agreement is also close to the line formed by using properties from reference 8. The significance of agreement between the n values as derived from flow and from critical pressure ratios is that it substantiates the reasonableness of assuming that the flow process follows $pv^n = c$. The same value of n , thereby, may be used in determining the critical flow conditions at the throat that are derivable on this basis (e.g., the critical velocity and the critical specific volume). The use of properties from reference 7 necessitates the use of a different value of n for each parameter.

Comparing the results in figure 7 with the expansion indexes for the theoretical equilibrium and supersaturated-frozen processes on the basis of critical pressure ratios, shown by the dashed lines, indicates that neither process is a reasonable model for the flow. The expansion index for the case of a supersaturated-equilibrium process falls reasonably close to the measured values and thus provides further evidence that this process may be the best model to represent the flow.

Effect of Superheat

The purpose of adding superheat in this investigation was primarily to observe any pronounced change in the flow that might provide a clue to the nature of the process through the nozzle. Based on the analysis in reference 1, initially saturated vapors will flow supersaturated to a point in the nozzle where condensation will suddenly begin and continue thereafter. The point of condensation depends on the inlet conditions. Below about 1500° F, the point is downstream of the throat and above this temperature is upstream of the throat, approaching the inlet as the saturation temperature is increased. Adding superheat at constant pressure reverses the effect, driving the condensation point downstream and with sufficient superheat to beyond the throat of the nozzle. The effect of the point of condensation having moved from upstream to downstream of the throat should be evident by a significant increase in the flow, if it is assumed that the process is essentially in equilibrium when the point of condensation is upstream and is essentially supersaturated-frozen when it is downstream. To determine the magnitude of the change that might be expected, a calculation was made at the nozzle inlet pressure corresponding to a saturation temperature of 1550° F. At the saturated condition, the supersaturated-frozen flow was about 7 percent higher than the equilibrium flow. At 100° of superheat, the flow decreased 1 percent for an equilibrium process and 3 percent for a supersaturated-frozen process. The net effect was to reduce the difference between the two processes by 2 percentage points so that the difference between the two processes at 100° of superheat is, therefore, about 5 percent, which should be readily observed.

The effects of superheat on the two processes are indicated in figure 8 by the straight lines originating at the saturated flow curves, which are shown for reference. Included in figure 8 are all of the averaged experimental flow

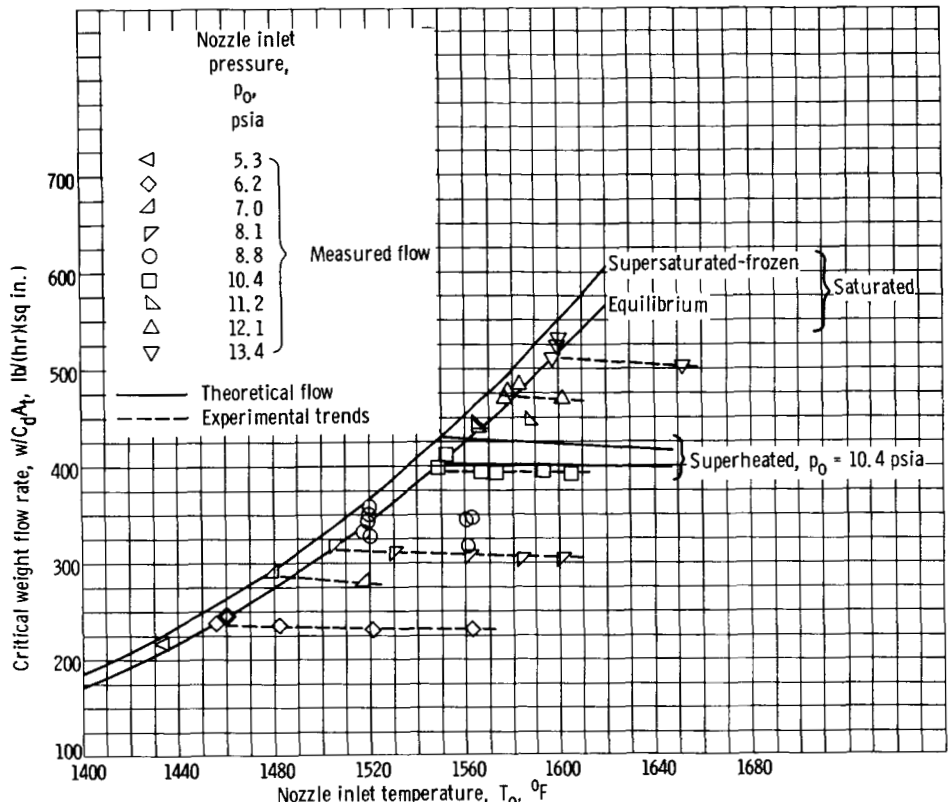


Figure 8. - Variation of critical vapor flow with nozzle inlet temperature.

data from table II (p. 9). For the experimental points, the nozzle inlet temperature is the sum of the separator temperature and the amount of superheat measured.

At an inlet condition of 8.8 pounds per square inch absolute, an irregular behavior in flow was experienced. With 40° of superheat applied, the condenser temperature was raised from 1205° to 1302° F (run 16). Subsequently, the flow decreased with each measurement at fixed inlet condition (runs 16 to 19). Upon removing the superheat, the flow increased but was inconsistent. Later in the test program (runs 53 to 54), the flow again showed a wide deviation at this nozzle inlet pressure with no superheat and with the condenser at 1255° F. A condenser temperature between 1302° and 1205° F should not be sufficient to unchoke the nozzle, which would explain the marked decrease in flow. No unusual behavior in the facility was observed that might account for the erratic behavior of the flow.

Below and above 8.8 pounds per square inch absolute, where there are sufficient points, the flow gradually decreases with superheat with no marked increase in flow. Either the superheat was insufficient, or the process is other than that of the nature assumed, possibly a supersaturated-equilibrium process as was shown plausible by the check with saturated flows.

SUMMARY OF RESULTS

Critical flow rates and pressure ratios of sodium vapor flow through an axisymmetrical convergent-divergent nozzle were measured to determine the characteristics of the expansion process. Flows at inlet pressures from approximately 5 to 13.5 pounds per square inch absolute (1425° to 1600° F) and temperatures with up to 100° of superheat were investigated. The measured flows, corrected for a flow coefficient of 0.97, were compared with theoretical one-dimensional isentropic flows obeying $pv^n = c$ where p is the absolute pressure, v is the specific volume, n is the expansion index, and c is a constant. Comparison of the measure flows with equilibrium and supersaturated-frozen flows, as well as a supersaturated-equilibrium flow, were also made. Expansion indexes derived from critical pressure ratios were compared with the values derived from flow. The effect of superheat on the characteristics of flow was noted. Three sources of data were considered to investigate the effect of differences in available thermodynamic properties on interpretation of results. The following results were found:

1. Over the range of inlet pressures investigated, the critical flows without superheat and corrected for a flow coefficient of 0.97 could be approximated by the straight line $w/C_d A_t = 39.4 p_0$ where w is the weight flow, C_d is the nozzle flow coefficient, A_t is the area of the nozzle throat, and p_0 is the nozzle inlet pressure. Deviations from this line were within ± 2 percent at pressures above 9 pounds per square inch absolute and as high as ± 5 percent at pressures below 9 pounds per square inch absolute.

2. The flows obtained experimentally agreed more closely with theoretical flows based on an equilibrium process than on a supersaturated process in the range of pressures investigated. A calculation of flow for a supersaturated-equilibrium process agreed very closely with the least-squares line for measured flows. The corresponding expansion index was close enough to those from critical pressure ratios measured to indicate this process as perhaps the most plausible.

3. The expansion index n derived from measured flows and based on $pv^n = c$ increased with nozzle inlet pressure and ranged in values of 1.18 to 1.28 at 5 pounds per square inch absolute and 1.3 to 1.4 at 13.5 pounds per square inch absolute, depending on the source of properties used. A nominal value of 1.3 over the range of pressures appeared to be reasonable. The values derived from measured critical pressure ratios agreed favorably with those derived from flow for two of the three property sources and indicated a similar increasing trend with inlet pressure.

4. Addition of superheat up to 100° did not cause a change in flow that could be attributed to a change in the nature of the process. The flow decreased gradually with increased superheat at any given pressure.

Lewis Research Center,
National Aeronautics and Space Administration,
Cleveland, Ohio, September 13, 1965.

REFERENCES

1. Glassman, Arthur J.: Analytical Study of the Expansion and Condensation Behavior of Alkali-Metal and Mercury Vapors Flowing Through Nozzles. NASA TN D-2475, 1964.
2. Coultas, T. A.: Thermodynamic Aspects of the Flow of Sodium Vapor Through a Supersonic Nozzle. Research Rept. No. 61-32, Rocketdyne Div., North American Aviation, Inc., Nov. 1961.
3. Nichols, Landon R.; Winzig, Charles H.; Nosek, Stanley M.; and Goldman, Louis J.: Design and Operational Performance of a 150-Kilowatt Sodium Flash-Vaporization Facility. NASA TN D-1661, 1963.
4. Nichols, Landon R.; Nosek, Stanley M.; Winzig, Charles H.; and Goldman, Louis J.: Experimental Determination of Sodium Vapor Expansion Characteristics with Inert-Gas-Injection Pressure-Measuring Technique. NASA TN D-2276, 1964.
5. Affel, R. G.; Burger, G. H.; and Pidgeon, R. E.: Level Transducers for Liquid Metals. Rept. No. ORNL 2792, Oak Ridge Nat. Lab., Apr. 28, 1960.
6. Dunning, E. L.: The Thermodynamic and Transport Properties of Sodium and Sodium Vapor. Rept. No. ANL-6246, Argonne Nat. Lab., Oct. 1960.
7. Sittig, Marshall: Sodium - Its Manufacture, Properties, and Uses. Reinhold Pub. Corp., 1956.
8. Makansi, M.; Selke, W. A.; and Bonilla, C. F.: Thermodynamic Properties of Sodium. J. Chem. Eng. Data, vol. 5, no. 4, Oct. 1960, pp. 441-452.
9. Meisl, C. J.; and Shapiro, A.: Thermodynamic Properties of Alkali Metal Vapors and Mercury. (Second Edition.) Rept. No. R60FPD358-A, General Electric Co, Nov. 9, 1960.
10. Evans, William H.; Jacobson, Rosemary; Munson, Thomas R.; and Wagman, Donald D.: Thermodynamic Properties of the Alkali Metals. Jour. Res. Nat. Bur. Standards, vol. 55, no. 2, Aug. 1955, pp. 83-96.
11. Stone, J. P.; Ewing, C. T.; Spann, J. R.; Steinkuller, E. W.; Williams, D. D.; and Miller, R. R.: High Temperature Properties of Sodium, Potassium, and Cesium. Rept. No. 6128, Naval Res. Lab., June 4, 1964.